Available online at www.sciencedirect.com
ScienceDirect
Polymer 49 (2008) 1748–1760
polymer
www.elsevier.com/locate/polymer

Synthesis and characterization of poly(pyridinium salt)s with oxyalkylene units exhibiting amphotropic liquid–crystalline and photoluminescence properties☆

Pradip K. Bhowmik*, Sumanvedi Kamatam, Haesook Han, Alexi K. Nedeltchev

Department of Chemistry, University of Nevada at Las Vegas, 4505 Maryland Parkway, Box 454003, Las Vegas, NV 89154-4003, USA

Received 5 December 2007; received in revised form 4 February 2008; accepted 12 February 2008
Available online 16 February 2008

Abstract

Several novel poly(pyridinium salt)s with oxyalkylene moieties in the main chain with bulky organic counterions (tosylate and triflimide) were prepared by either the ring-transmutation polymerization of phenylated bis(pyrylium tosylate) salt with a series of oxyalkylene containing diamines in dimethyl sulfoxide on heating for 48 h or the metathesis reaction of the corresponding tosylate polymers with lithium triflimide in methanol. Their chemical structures were determined by elemental analysis and ^{1}H and ^{13}C NMR spectroscopies, and their polyelectrolyte behavior in dimethyl sulfoxide was determined by solution viscosity measurements. Their weight average molecular weights were in the range 14,000–22,000 and polydispersity indices were in the range 1.20–1.70 as determined by gel permeation chromatography. They were characterized both for their thermotropic and lyotropic liquid–crystalline properties by using differential scanning calorimetry and polarizing optical microscopy. Since these polymers exhibited liquid–crystalline phase both in the melt and in solution, they can be appropriately classified as amphotropic class of ionic polymers. Their light-emitting properties were also determined by using spectrofluorometry.

Keywords: Ionic liquid–crystalline polymers; Amphotropic; Photoluminescence

1. Introduction

π-Conjugated polymers such as poly(*p*-phenylene vinylene) (PPV), poly(*p*-phenylene) (PPP), poly(*p*-phenylene ethynylene) (PPE), polyfluorene (PF), and polythiophene (PT) exhibit many interesting properties including the emission of light in the entire visible region of the electromagnetic spectrum [1–3]. However, because of the presence of highly π-conjugated aromatic rings in their chemical structures, they are usually insoluble in known solvents and decompose before their melting transitions. Therefore, they impart a serious problem to process them for making useful devices. Either to make them soluble in suitable solvents or to make them low melting transitions so that they can be processed in the melt, several chemical structural modifications are required to address the problems usually associated with this class of polymers. One of the important chemical modifications is to incorporate flexible oxyethylene units in the side chain [4–7] or in the backbones of the π-conjugated polymers [8–10], although in the latter case the polymers are no longer considered as fully conjugated systems. This class of polymers can derive their interesting properties from the conjugated segments along with their solubility in common organic solvents because of the presence of oxyethylene units which make them interesting polymers to study the structure–property–application relationships. For example, PFs with oxyethylene side chains have been prepared by Ni(0) coupling reaction. The oxygenated side chains enable them to bind with metal ions, making them suitable as emissive materials for blue-emitting light-emitting electrochemical cells (LECs) as well as light-emitting devices (LEDs). Their light emission in

☆ This article is dedicated to Professor Donald W. Boerth with best wishes on the occasion of his 60th birthday.

* Corresponding author. Tel.: +1 702 895 0885; fax: +1 702 895 4072.
E-mail address: pradip.bhowmik@unlv.edu (P.K. Bhowmik).

0032-3861/$ - see front matter © 2008 Elsevier Ltd. All rights reserved.
doi:10.1016/j.polymer.2008.02.021

both LED and LED devices rapidly changes from blue ($\lambda_{max} = 430$ nm) to blue-green due to the appearance of long-wavelength emission centered at 530 nm [4].

Both thermotropic and lyotropic LC phases are usually observed for polymers with rigid backbones. π-Conjugated polymers might, therefore, be expected to behave in a similar manner. Thermotropic LC phases have been studied extensively for PFs–π-conjugated polymers. Poly(9,9-dioctylfluorene) exhibits LC phase in the melt between 170 and 270 °C and poly(9,9-di(ethylhexyl)fluorene) exhibits LC phase above 167 °C. The LC phases are birefringent but the textures observed do not provide an unambiguous identification of the phase. The texture is retained into a glassy state when it was rapidly cooled, indicating that the polymer orientation is retained without crystallization. Quenching from the LC phase of films on polyimide LC alignment layers also results in oriented monodomains [11,12].

In this article, we describe the synthesis of a series of poly(pyridinium salt)s containing flexible oxyalkylene units in the backbones and organic counterions, and the characterization of their lyotropic and thermotropic properties. The chemical structures and designations of these ionic polymers, **I-1**–**I-3** and **II-1**–**II-3**, which are prepared and characterized, are shown in Scheme 1. Because of the presence of flexible oxyalkylene units and organic counterions in these polymers, their solubility in common organic solvents might exceed the critical concentration (C^*) to form lyotropic LC phases in various organic solvents. Development of this class of polymers having lyotropic properties in common organic solvents was the one principal objectives since there are a limited number of ionene polymers that exhibit lyotropic LC phases in organic solvents in the literature [13–21]. They were also targeted to have low crystal–LC phase transitions for their thermotropic properties because of the flexible units present in their backbones. Again, there are many ionic polymers reported in the literature, but there exist a limited number of ionic polymers that exhibit thermotropic LC properties [19,21,22–28]. Therefore, development of ionic polymers having thermotropic properties was another goal in this study. Their light-emitting properties in solutions of various organic solvents and in the solid state were also included. The three important and other relevant properties of these polymers were examined by several experimental techniques including viscometry, gel permeation chromatography (GPC), polarizing optical microscopy (POM), differential scanning calorimetry (DSC), thermogravimetric analysis (TGA), UV–vis spectrophotometry, and photoluminescence spectrometry.

2. Experimental section

2.1. Monomer synthesis

4,4′-(1,4-Phenylene)bis(2,6-diphenylpyrylium)ditosylate, **M**, was synthesized by using the procedure described in the literature [16]. The three aliphatic diamines, 2,2′-oxybis(ethylamine) (95% pure), 1,2-bis(2-aminoethoxy)ethane (97% pure), and 4,9-dioxy-1,12-dodecadiamine (97% pure) were received from TCI and used as-received to prepare polymers **I-1**–**I-3**, respectively. The $LiN(O_2SCF_3)_2$ salt was purchased from Sigma–Aldrich Chemical Co. and used without further purification for the metathesis reaction to prepare polymers **II-1**–**II-3**.

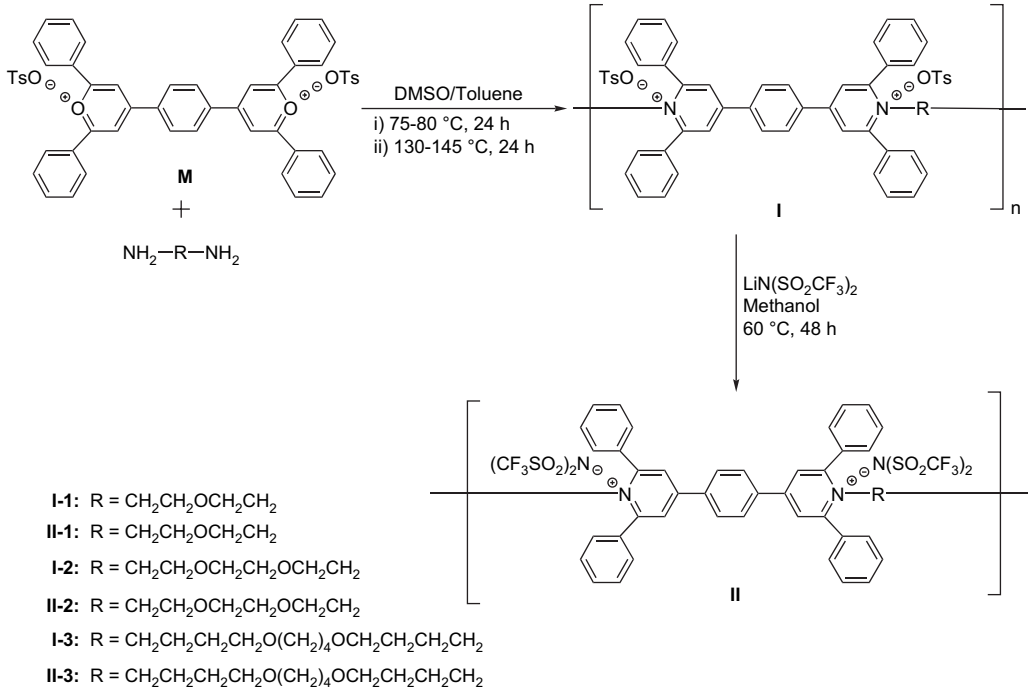

Scheme 1.

2.2. Polymer synthesis

2.2.1. Synthesis of polymers *I-1–I-3*

The bis(pyrylium salt) **M** (4.64 g, 5.25 mmol) was polymerized with 2,2′-oxybis(ethylamine) (0.57 g, 5.25 mmol) by ring-transmutation polymerization [16] reaction to yield polymer **I-1** that was carried out at initially 75–80 °C for 24 h and then 130–145 °C for additional 24 h in DMSO as shown in Scheme 1. The water generated during the polymerization was distilled off as a toluene/water azeotrope. The polymer was isolated in good yield by precipitation from water and washed repeatedly with large quantity of water. Additionally, it was stirred in water at room temperature (rt) overnight to remove residual DMSO that was embedded in the polymer matrix. It was then dried *in vacuo* for 3 days at 80–85 °C to afford 3.8 g (yield 76%). Anal. Calcd for $C_{58}H_{50}N_2O_7S_2$ (**I-1**): C, 73.24; H, 5.30; N, 2.95; S, 6.74. Found: C, 71.92; H, 5.59; N, 3.16; S, 6.16.

Similarly, polymers **I-2** and **I-3** were prepared by ring-transmutation polymerization reaction of bis(pyrylium)salt **M** (4.63 g, 5.02 mmol and 4.09 g, 4.64 mmol) with the corresponding 1,2-bis(2-aminoethoxy)ethane (0.74 g, 5.02 mmol) and 4,9-dioxy-1,12-dodecadiamine (1.11 g, 4.64 mmol) to yield 3.5 g (71%) and 3.9 g (78%), respectively, under essentially identical conditions.

*Selected data for (**I-2**).* δ_H (DMSO-d_6, 400 MHz, ppm): 8.36–8.60 (4H, s, aromatic *meta* N^+), 7.50–8.34 (24H, m, aromatic), 7.43–7.45 (4H, d, $J = 8$ Hz, tosylate), 7.05–7.07 (4H, d, $J = 8$ Hz, tosylate), 4.53 (4H, s, $^+N-CH_2$), 3.11 (4H, s, CH_2-O), 2.78 (4H, s, $O-CH_2CH_2-O$), and 2.24 (6H, s, CH_3); δ_C (DMSO-d_6, 100 MHz, ppm): 157.00, 153.09, 146.13, 137.87, 137.87, 136.60, 133.39, 131.25, 130.11, 130.05, 129.98, 129.77, 129.59, 128.35, 127.40, 126.70, 125.86, 69.41, 67.62, 54.10, 21.12. Anal. Calcd for $C_{60}H_{54}N_2O_8S_2$: C, 72.41; H, 5.47; N, 2.81; S, 6.44. Found: C, 70.56; H, 6.35; N, 2.97; S, 6.37.

*Selected data for (**I-3**).* δ_H (DMSO-d_6, 400 MHz, ppm): 8.48–8.58 (4H, s, aromatic *meta* N^+), 7.50–8.38 (24H, m, aromatic), 7.43–7.45 (4H, d, $J = 8$ Hz, tosylate), 7.06–7.08 (4H, d, $J = 8$ Hz, tosylate), 4.41 (8H, m, $^+N-CH_2CH_2-$), 2.80–2.92 (16H, s, $O-CH_2CH_2-$), and 2.25 (6H, s, CH_3); δ_C (DMSO-d_6, 100 MHz, ppm): 157.06, 156.61, 152.82, 146.13, 137.84, 136.60, 133.46, 131.29, 130.06, 129.97–129.12, 128.43, 127.38, 126.77, 125.80, 69.49, 66.55, 53.10, 29.27, 25.80, 25.75, 21.10. Anal. Calcd for $C_{66}H_{66}N_2O_8S_2$: C, 73.44; H, 6.16; N, 2.60; S, 5.94. Found: C, 73.09; H, 6.25; N, 2.84; S, 6.00.

2.2.2. Synthesis of polymers *II-1–II-3*

Polymer **II-1** was prepared by the metathesis reaction of polymer **I-1** with lithium triflimide in a common organic solvent such as methanol [16]. The procedure that was employed was described as follows: polymer **I-1** (1.7 g, 1.7 mmol) was dissolved in 40 mL of methanol on gentle warming. To the methanol solution of this polymer, 20 mL of methanol solution of lithium triflimide (1.0 g, 3.5 mmol) was added dropwise on stirring. The resulting solution was kept at 60 °C for 72 h with vigorous stirring. After removing methanol by a rotary evaporator, the viscous solution was poured into a beaker containing distilled water to dissolve both lithium tosylate and excess lithium triflimide, affording the desired solid polymer **II-1**. It was collected by filtration and washed several times with a large quantity of distilled water. These procedures were repeated for at least one more time to ensure that the tosylate counterions were completely exchanged by the triflimide counterions in the polymer (monitored by ^1H NMR spectrum). Then it was dried *in vacuo* at 80–85 °C for 3 days and weighted to give 1.8 g (yield 91%) of polymer **II-1**. Anal. Calcd for $C_{48}H_{36}N_4O_9F_{12}S_4$ (**II-1**): C, 49.32; H, 3.10; N, 4.79; S, 10.97. Found: C, 51.58; H, 3.42; N, 4.48; S, 10.00.

Similarly, polymers **II-2** and **II-3** were prepared by the metathesis reaction of the corresponding polymers **I-2** (1.7 g, 1.7 mmol) and **I-3** (1.9 g, 1.7 mmol) with lithium triflimide (1.0 g, 3.5 mmol and 1.0 g, 3.5 mmol) to yield 1.8 (90%) and 2.0 g (93%), respectively, by using the identical procedure that was adopted for polymer **II-1**.

*Selected data for (**II-2**).* δ_H (DMSO-d_6, 400 MHz, ppm): 8.45–8.60 (4H, s, aromatic *meta* N^+), 7.51–8.36 (24H, m, aromatic), 4.53 (4H, s, $^+N-CH_2$), 3.11 (4H, s, CH_2-O), and 2.78 (4H, s, $O-CH_2CH_2-O$); δ_C (DMSO-d_6, 100 MHz, ppm): 157.40, 153.50, 136.92, 135.85, 131.57, 130.55–130.09, 129.87, 129.67, 127.12–127.07, 124.95, 122.38, 121.74, 118.54, 115.33, 69.72, 67.80, 54.38. Anal. Calcd for $C_{50}H_{40}N_4O_{10}F_{12}S_4$: C, 49.51; H, 3.32; N, 4.62; S, 10.57. Found: C, 51.72; H, 4.13; N, 4.62; S, 10.13.

*Selected data for (**II-3**).* δ_H (DMSO-d_6, 400 MHz, ppm): 8.48–8.60 (4H, s, aromatic *meta* N^+), 7.52–8.37 (24H, m, aromatic), 4.41 (8H, m, $^+N-CH_2CH_2-$), 2.80–2.92 (16H, s, $O-CH_2CH_2-$); δ_C (DMSO-d_6, 100 MHz, ppm): 157.42, 156.93, 153.24, 139.32, 136.95, 133.58, 131.60, 130.60, 129.95–129.70, 127.71, 126.13, 124.95, 121.75, 118.54, 115.34, 69.80, 66.80, 53.40, 29.67, 29.44, 26.10. Anal. Calcd for $C_{56}H_{52}N_4O_{10}F_{12}S_4$: C, 51.85; H, 4.04; N, 4.32; S, 9.89. Found: C, 52.22; H, 4.30; N, 4.43; S, 9.50.

2.3. Polymer characterization

The ^1H and ^{13}C NMR spectra of the poly(pyridinium salt)s, **I-1–I-3** and **II-1–II-3** were recorded with a Varian 400 MHz VnmrJ.2.1A spectrometer with three RF channels operating at 400 and 100 MHz, respectively, in DMSO-d_6 using TMS as an internal standard. Their solutions were prepared by dissolving ca. 20 mg of specific polymer in DMSO-d_6 with tetramethylsilane (TMS) as an internal standard. Inherent viscosities (IVs) of the polymers were measured in DMSO at various concentrations (0.02–0.10 g/dL) with a Cannon Ubbelohde viscometer #75 J394 at 35 °C to determine their polyelectrolyte behavior. Gel permeation chromatography (GPC) was performed for the synthesized polymers in DMSO at 70 °C with a flow rate 1.0 mL/min with a Waters 515 pump together with a Viscotek Model 301 Triple Detector Array that combines a laser refractometer, a differential viscometer, and an RALS/LALS detector in a single instrument with fixed interdetector volumes and temperature control to 80 °C. Although

conventional chromatographic calibrations are not required for this type of GPC instrument, the pullulan standards of P-10 and P-50 from Polymer Standards Services USA, Inc. were used for the instrument calibration. Separations were accomplished using ViscoGel I-MBHMW-3078 columns from Viscotek. A 100 μL of 0.2 wt% of polymer in DMSO containing 0.01 M LiBr was injected into the columns. Data analyses were performed using Viscotek TriSEC software.

Phase transition temperatures were measured with a TA 2100 differential scanning calorimeter under a nitrogen flow at heating and cooling rates of 10 °C/min. The temperature axis of the DSC thermogram was calibrated before use with the reference standard of high-purity indium and tin. Polymers usually weighing 4–6 mg were used for this analysis. The thermogravimetric analysis (TGA) was performed with a TA 2100 instrument at a heating rate of 10 °C/min in nitrogen.

Both thermotropic and lyotropic liquid–crystalline properties of the polymers were studied using a polarized optical microscopy (POM, Nikon, Model Labophot 2) equipped with crossed polarizer and a hot stage. Samples of these ionene polymers for lyotropic properties were made by dissolving known amounts of polymers into known amounts of specific solvents.

Absorption spectra for the polymer solutions were studied in various spectrograde solvents such as dimethyl sulfoxide (DMSO), acetonitrile (CH_3CN), methanol (CH_3OH), chloroform ($CHCl_3$), acetone, and tetrahydrofuran (THF) by using Varian Cary 3 Bio UV–vis spectrophotometer at ambient temperatures. Their photoluminescence spectra in solution and solid states were examined with Perkin–Elmer LS55 spectrophotometer with a xenon lamp light source at ambient temperature. The polymer solutions to examine their spectra were prepared by dissolving the polymers in suitable solvents and the solvent cast thin films were prepared by placing the polymer solutions on quartz slides and allowed them to dry in vacuum oven to evaporate the solvents.

3. Results and discussion

3.1. Chemical structures

The elemental analysis results are consistent with the proposed structures of all polymers, since theoretical percentages of different elements in the polymers are in good agreement with the experimental values. All the ^{1}H and ^{13}C NMR spectra recorded for polymers **I-1**–**I-3** and **II-1**–**II-3** are also in excellent agreement with their proposed structures. As representative examples the ^{1}H and ^{13}C spectra of polymers **I-1** and **II-1** are shown in Figs. S1 and S2. In Fig. S1a, the ^{1}H NMR spectrum of polymer **I-1** contained the aromatic and the pyridinium ring absorptions between 7.44 and 8.52 ppm, the tosylate aromatic absorptions between 7.02 (d, $J = 8$ Hz) and 7.42 (d, $J = 8$ Hz) ppm, the methyl protons of tosylate absorptions at 2.21 ppm, and the protons from oxyethylene group absorptions between 2.74 ($^+NCH_2$) and 4.30 ($-OCH_2$) ppm. According to the mechanism for the conversion of pyrylium salt to the pyridinium salt [29] the last ring closing step involves a nucleophilic attack of a vinylogous amino group on a carbonyl group and is followed by the loss of a water molecule. The proton signals of vinylogous amide and amino end groups were not detected in its ^{1}H NMR spectrum. Additionally, its ^{13}C NMR spectrum contained only aromatic carbon signals between 126.12 and 157.43 ppm. The carbonyl resonance at ca. 186.70 ppm, which is attributable to a vinylogous amide [30], was not detected suggesting that the ring-transmutation polymerization reaction proceeded to completion. In Fig. S2a, the ^{1}H NMR spectrum of polymer **II-1** contained the aromatic and the pyridinium ring absorptions between 7.42 and 8.59 ppm, and the protons from oxyethylene group absorptions between 2.77 ($^+NCH_2$) and 4.31 ($-OCH_2$) ppm. The absence of tosylate proton absorptions (both the tosylate aromatic and the methyl proton absorptions) suggested that exchange of tosylate ion with triflimide was effective in the metathesis reaction under the experimental conditions used. Its ^{13}C NMR spectrum contained the aromatic carbon signals between 114.06 and 157.42 ppm and aliphatic carbon signals at 53.65 ($^+NCH_2$) and 67.77 ($-OCH_2$) ppm.

3.2. Dilute solution properties

The polyelectrolyte behaviors of polymers **I-1**–**I-3** and **II-1**–**II-3** were tested in DMSO by measuring the inherent viscosities of dilute polymer solutions [31–40]. The polymers **I-1** and **II-1** did not exhibit a typical polyelectrolyte behavior. Polymer **II-2** showed the lowest increase in inherent viscosity with decreasing polymer concentrations. Polymer **I-2** exhibited two peaks with maxima in inherent viscosities at very dilute concentrations of 0.04 and 0.08 g/dL. Such peaks with an increase in inherent viscosities made it difficult to extrapolate the inherent viscosity to $c = 0$ and determine its intrinsic viscosity, $[\eta]$. The maximum in the plot of inherent viscosity vs polymer concentration is known as abnormal viscosity behavior reported in the literature not only for flexible polyelectrolytes but also for rigid-rod polyelectrolytes in water [38]. Despite the presence of flexible oxyalkylene moieties, polymers **I-1**–**I-3** and **II-1** and **II-2** did not obey the empirical Fuoss equation [31,32]. Unlike polymers **I-1**–**I-3** and **II-1** and **II-2**, polymer **II-3** exhibited a typical polyelectrolyte behavior in DMSO, that is, its inherent viscosity increased with the decrease in polymer concentration (Fig. 1a) and the intrinsic viscosity, [η], was found to be 4.4×10^{-3} dL/g by extrapolating the inherent viscosity to $c = 0$ (Fig. 1b). It also obeyed the empirical Fuoss equation [31,32], which is usually applied to random coiled polyelectrolytes: $\eta_{inh} = A/(1 + Bc^{0.5}) \Rightarrow (\eta_{inh})^{-1} = 1/A + B/Ac^{0.5}$, where A and B are constants; η_{inh} and c are usual notations. It is known that a characteristic of a polyelectrolyte is the chain extension thus resulting in large hydrodynamic volume that occurs in water or polar organic solvent at low concentrations [38]. This effect is due to Columbic repulsions between charged groups along the polymer chain, forcing the polymer into an extended, rod-like conformation. The addition of salt to a polyelectrolyte solution or change in pH of polyelectrolyte solution screens the repulsive electrostatic interactions, and the

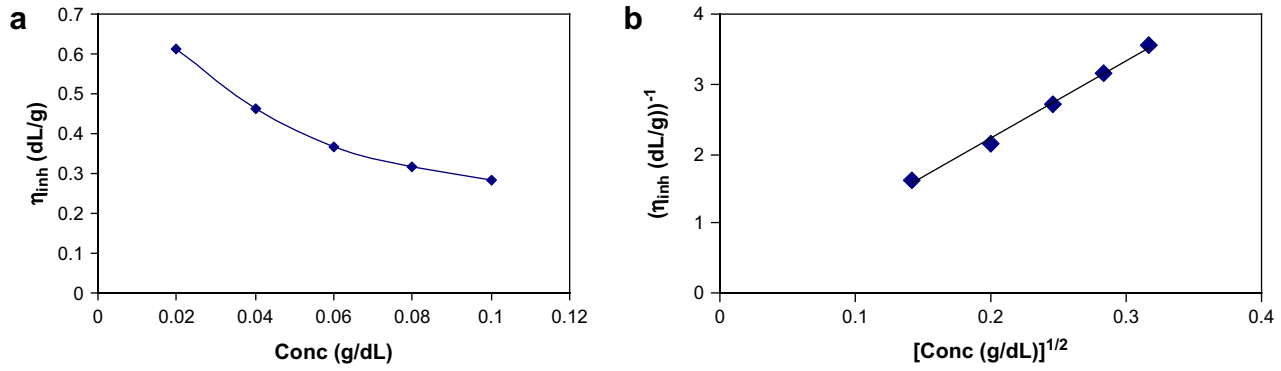

Fig. 1. (a) Polyelectrolyte behavior and (b) Fuoss plot of polymer **II-3** in DMSO at 35 °C.

polymer chain shrinks, adopting a more entropically favored conformation. This is known as the polyelectrolyte effect [31–40].

3.3. Gel permeation chromatography of polymers

As representative examples, the gel permeation chromatographs (GPCs) of polymers **I-2** and **II-2** obtained by using a Viscotek TDA instrument are shown in Fig. 2.

Overall, inter-detector signals, that is, refractometer, viscometer and right angle laser light scattering (RALS) signals are quite satisfactory with the exception of the fact that signal-to-noise of RALS signal is less than perfect. Note here that RALS signals for low molecular weight polymers (10,000–25,000) are always less than perfect. The data obtained from GPC studies of synthesized polymers are compiled in Table 1. These data indicated that they had intrinsic viscosities in the range 0.05–0.12 dL/g, number average molecular weights (M_ns) in the range 10,000–15,000, weight average molecular weights (M_ws) in the range 14,000–22,000 and polydispersity indices in the range 1.20–1.70. As expected, the molecular weights and polydispersity indices of the tosylate and triflimide polymers are essentially in the similar range, since triflimide polymers were synthesized by the metathesis reactions of tosylate polymers with lithium triflimide salts [16].

3.4. Solubility of polymers in organic solvents

The solubilities of the synthesized polymers **I-1**–**I-3** and **II-1**–**II-3** in various organic both polar and nonpolar solvents were examined revealing that their solubilities in several organic solvents were increased significantly as opposed to the poly(pyridinium salt)s with inorganic tetrafluoroborate counterions (Table 2) [41,42]. The organic tosylate and triflimide counterions reduce the electrostatic interactions between the pyridinium ions present in the polymer chain and the counterions due to their significant delocalization of polarizable electron clouds. Since the counterions are loosely bound through developing covalent character (more organic-like) that allows organic solvent molecules to interact with the polymers more readily. The polymers **I-1**–**I-3** swelled in acetone and tetrahydrofuran, but the polymers **II-1**–**II-3** were soluble in these two solvents. Generally, swelling of the polymers is a slow process, which involves the penetration of solvent molecules into the polymer matrix thereby increasing its mass and volume. In the swelling phenomenon, the solvent cannot dissolve the polymer to make solution but they have limited interaction with a given solvent. Polymers **I-1**–**I-3** and **II-1**–**II-3** showed excellent solubility in dimethyl sulfoxide, and also good solubility in methanol and acetonitrile. In particular, the polymers containing tosylate counterions (**I-1**–**I-3**) were more soluble in methanol whereas polymers having triflimide counterions (**II-1**–**II-3**) were more soluble in acetonitrile.

3.5. Lyotropic liquid–crystalline properties

The excellent solubility of polymers **I-1**–**I-3** and **II-1**–**II-3** in protic and aprotic organic polar solvents having the dielectric constants within the range 32.6–48.9 motivated us to examine their lyotropic properties in these solvents. The solution properties of polymer **I-1** in aprotic polar solvent acetonitrile ($\varepsilon = 37.5$) are shown in Table 3. Similar to several poly(pyridinium salt)s that exhibit lyotropic LC phase in both protic and aprotic polar solvents [13,15–17], it usually formed an isotropic solution at a low concentration up to 10 wt% in this solvent. At an intermediate concentration (C^*) (20–60 wt%), a biphasic solution formed in which an LC phase coexisted with an isotropic phase, which could not be separable even on prolonged standing. With the further increase in its weight percentage, the development of the LC phase increased with the expense of an isotropic phase in this solvent, which is essentially similar to poly(pyridinium salt)s [13,15–17] as well as many neutral lyotropic polymers in general [43]. At high concentration (71 wt%) it formed a fully-grown lyotropic phase in this solvent. On application of pressure or shear to a lyotropic phase, it caused the LC domains to deform, break, and coalesce into new ones, revealing the mobile nature of this phase. Additionally, at a higher concentration a more viscous but shearable gel resulted for this polymer. As a representative example, the photomicrographs of polymer **I-1** at 49 and 80 wt% in acetonitrile when viewed with a POM under crossed polarizers at room temperature are shown in Fig. 3, indicating its biphasic and lyotropic solutions, respectively. Interestingly

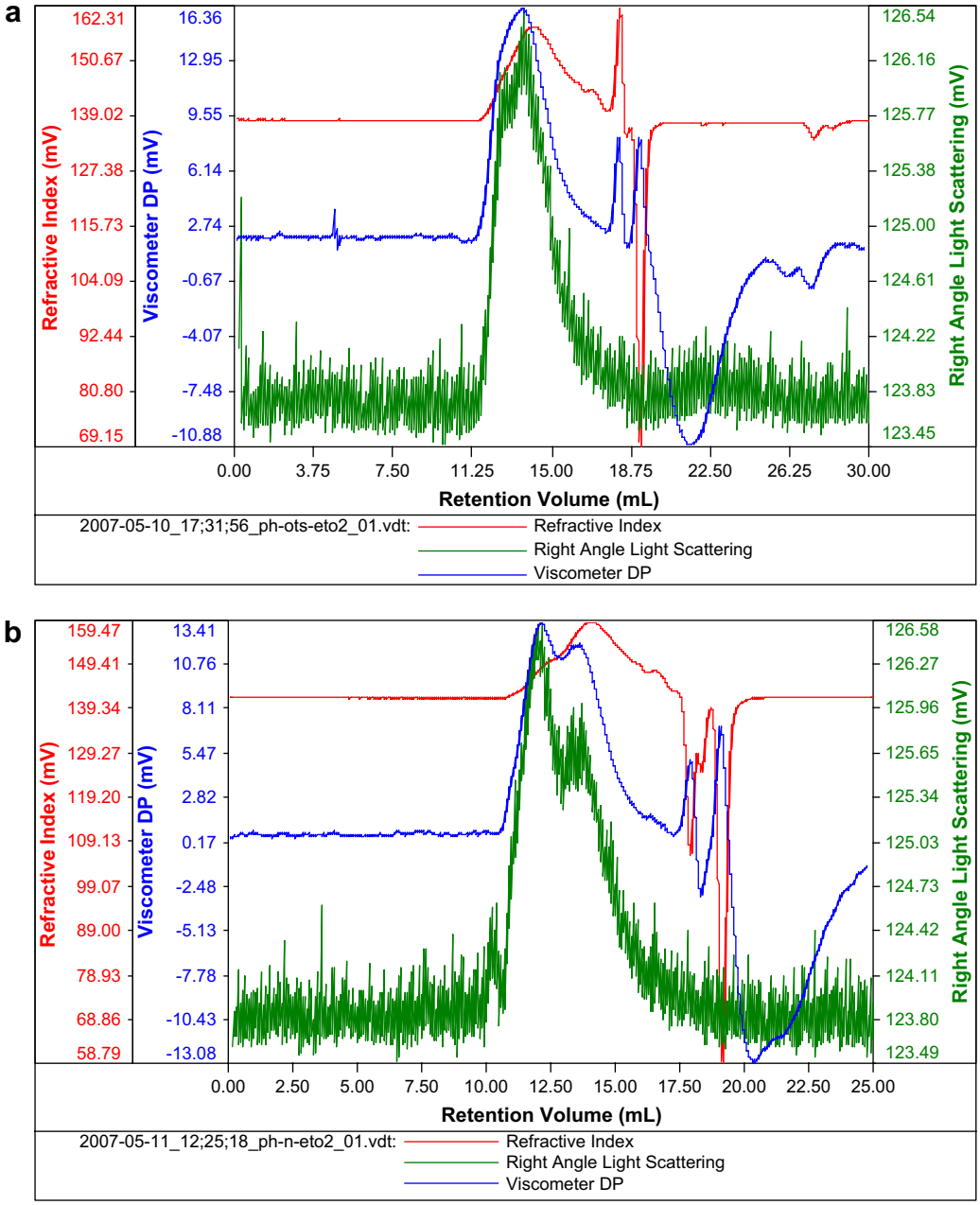

Fig. 2. Gel permeation chromatographs of (a) polymer **I-2** and (b) polymer **II-2**.

enough, one was able to draw a fiber manually by using a viscous gel of lyotropic phase of this polymer with a pair of tweezers (Fig. 4) wherein the polymer chain alignment and lyotropic phase are clearly visible. These high concentration values of polymer **I-1** in acetonitrile were indicative of the high degree of alignment of polymer chains required in solutions for the lyotropic phase to be observed.

The textures of lyotropic LC phases of compounds or polymers are more or less similar to thermotropic LC phases of

Table 1
GPC data for polymers **I-1**–**I-3** and **II-1**–**II-3**

Polymer	IV (dL/g)	M_n	M_w	M_w/M_n
I-1	0.08	11,816	14,280	1.2
II-1	0.05	15,395	22,134	1.4
I-2	0.12	10,763	14,818	1.4
II-2	0.12	13,229	22,490	1.7
I-3	0.08	15,436	18,638	1.2
II-3	0.10	11,342	18,223	1.6

Table 2
Solubility of polymers **I-1**–**I-3** and **II-1**–**II-3** in various organic solvents

	DMSO	CH_3OH	CH_3CN	Acetone	THF
I-1	+	+	+	Swelling	Swelling
II-1	+	+	+	+	+
I-2	+	+	+	Swelling	Swelling
II-2	+	+	+	+	+
I-3	+	+	+	Swelling	Swelling
II-3	+	+	+	+	+

The symbol '+' indicates that the polymer is soluble.

Table 3
Solution properties of polymer **I-1** in acetonitrile ($\varepsilon = 37.5$) at room temperature

Solvent	Concentration (wt%)	Solution properties[a]
CH_3CN ($\varepsilon = 37.5$)	5	Isotropic solution
	10	Isotropic solution
	20	Biphasic solution[b]
	31	Biphasic solution[b]
	49	Biphasic solution[b]
	59	Biphasic solution[b]
	71	Lyotropic solution[c]

[a] Observation with a polarizing light microscope between crossed polarizers at room temperature.
[b] Lyotropic phase coexisting with an isotropic phase.
[c] Strong shear birefringence.

compounds or polymers. However, the thermotropic systems have an advantage of being one-component systems and, hence less complex than the lyotropic compounds or polymers that are by definition many-component systems [44]. The lyotropic phases of compounds or polymers in specific solvents may exhibit the various textures of nematic, hexagonal (middle) and lamellar (neat) phases. The latter two phases are originally found in many amphiphilic compounds [44–46]. The textures observed with POM studies for all of the biphasic and lyotropic solutions of polymer **I-1** in acetonitrile indicated small and large bâtonnets, and different types of polygonal arrays (often referred to as mosaic textures) (Figs. 3 and 4), all of which were indicative of their lamellar phase [44–47].

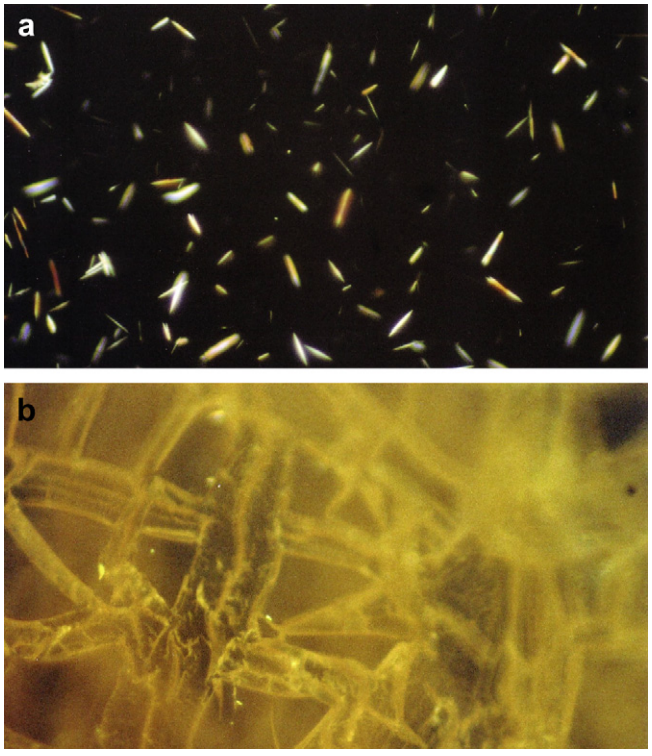

Fig. 3. Photomicrographs of polymer **I-1** at (a) 49 wt% in CH_3CN and (b) 80 wt% in CH_3CN under crossed polarizers exhibiting biphasic and lyotropic LC phases, respectively (magnification 400×).

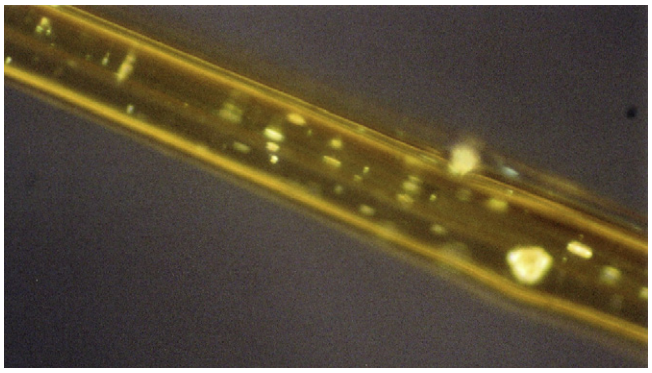

Fig. 4. Photomicrograph of a hand-drawn fiber obtained from polymer **I-1** at 71 wt% in CH_3CN exhibiting both alignment of polymer chain and lyotropic LC phase inside the fiber (magnification 400×).

An important feature of polymer **I-1** was that the textures of either the biphasic or the lyotropic solutions in acetonitrile were preserved on slow evaporation of this solvent from these solutions. Their basic features, that is, threaded textures mixed with small or large bâtonnets, and polygonal arrays, indicated that the local orientation of LC forming units in this polymer did not change when the slow evaporation of solvent occurred from either biphasic solutions or lyotropic solutions. However, they underwent a decrease in the density of threads with the simultaneous development of birefringent domains that presumably occurred because of the annihilation process between disclinations of various strengths and types. Finally, it underwent a time-dependent transition, from its biphasic or lyotropic solutions to a crystalline phase of spherulitic structures [14,18–21].

Despite the excellent solubility of polymer **I-1** in methanol (as high as 60 wt%) and dimethyl sulfoxide, the development of LC textures did not occur from these viscous solutions even on shearing, which precluded the observation of lyotropic phase in these solvents. Similarly, other polymers **I-2** and **I-3** and **II-1**–**II-3** had high solubility in methanol, acetonitrile and dimethyl sulfoxide, but the identification of lyotropic LC phases in these solvents was quite difficult because of very viscous gels. For example, viscous gels of polymers **I-2** and **I-3** and **II-1**–**II-3** could be prepared by using as high as 80 wt% in acetonitrile. Similarly, viscous gels of polymers **I-2** and **I-3** and **II-1**–**II-3** could also be prepared by using as high as 70 wt% in DMSO. Because of the difficulty in the preparation of thin films from highly viscous solutions hindered the development LC textures, the well-developed textures in LC polymers usually occur in thin films under crossed polarizers. Their high solubility in various polar solvents was related to the high solvophilic effects of these solvents with the pyridinium ions in conjunction with oxyethylene units present along the backbones of these polymers.

3.6. Thermotropic liquid–crystalline properties

Fig. 5a shows the DSC thermograms of polymer **I-1** obtained at heating and cooling rates of 10 °C/min. In the first

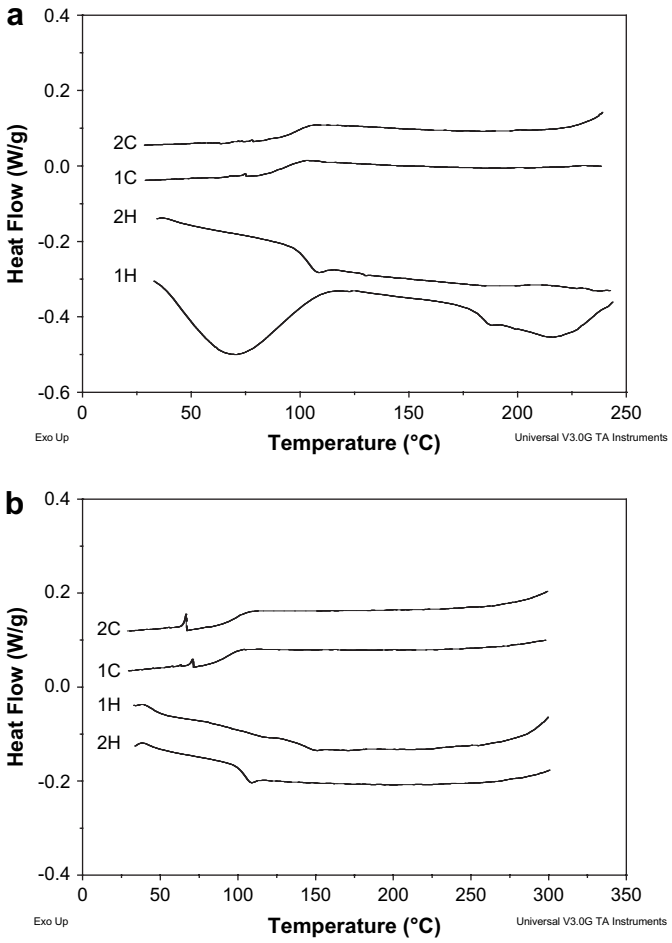

Fig. 5. DSC thermograms of (a) polymer **I-1** and (b) polymer **II-1** obtained at heating and cooling rates of 10 °C/min.

heating cycle, it showed a broad glass transition (T_g), a very small endotherm ($\Delta H = 0.09$ kcal/mol of the repeating unit) with a peak maximum at 186 °C and a broad endotherm with a peak maximum at 245 °C. In the subsequent cooling cycle, there were no cooling exotherms, but only a T_g at 98 °C. In the second heating cycle there was a distinct, single T_g at 104 °C, but no other endotherms. Like in the first cooling cycle, there was also a single T_g at 88 °C in the second cooling cycle. The variation of T_g values in the heating and cooling cycles suggested that its T_g was strongly dependent on its thermal history. In conjunction with POM studies, it was established that the small endotherm at 186 °C in the first heating cycle corresponded to the crystal-to-LC phase (T_m), since it exhibited highly birefringent, mobile phase (Fig. 6a) indicative of its LC phase. The broad endotherm in the first heating cycle corresponded to the LC-to-isotropic transition (T_i), which was verified by the observation of dark background at ca. 250 °C under the crossed polarizers. Fig. 6b shows a photomicrograph taken near the T_i at 245 °C revealing the dark spots. It had a temperature range of LC phase, that is, difference between T_m and T_i, of ca. 64 °C. Furthermore, the T_i of this polymer was also near to the decomposition temperature (T_d) at 252 °C obtained at a heating rate of 10 °C/min in

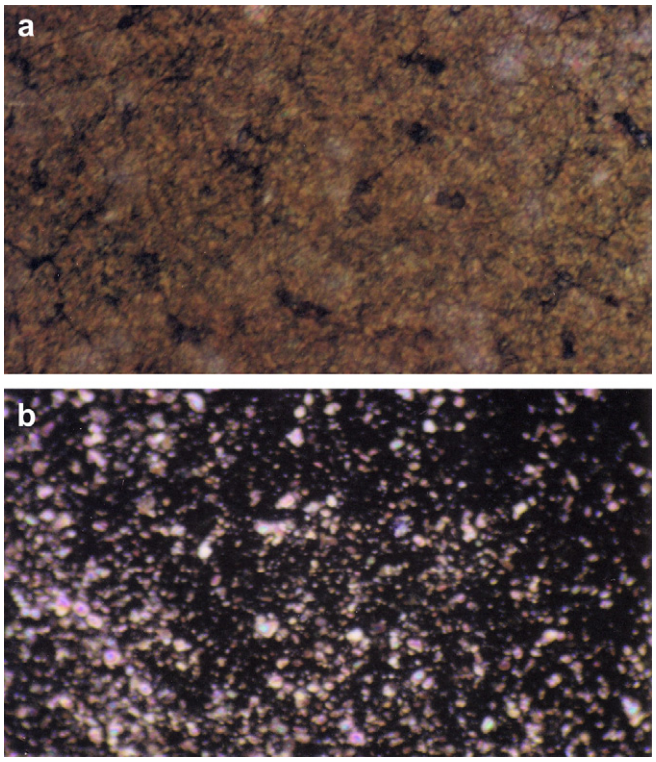

Fig. 6. Photomicrographs of polymer **I-1** taken at (a) 190 °C and (b) 245 °C under crossed polarizers exhibiting smectic LC phases (magnification 400×).

nitrogen by TGA measurement at which 5% weight loss of polymer **I-1** occurred (Fig. 7). Its T_m value was marginally higher than that (182 °C) of an analogous polymer containing 9 methylene units in the main chain [23], but much higher than that (116 °C) of an analogous polymer containing 12 methylene units in the main chain [24]. Note here that poly(pyridinium salt)s with either tetrafluoroborate or triflate as counterions do not exhibit thermotropic LC properties because of their thermal decomposition prior to melting transitions [22,23]. Thus, it was found that the tosylate ions as organic counterions in combination with oxyethylene units in the

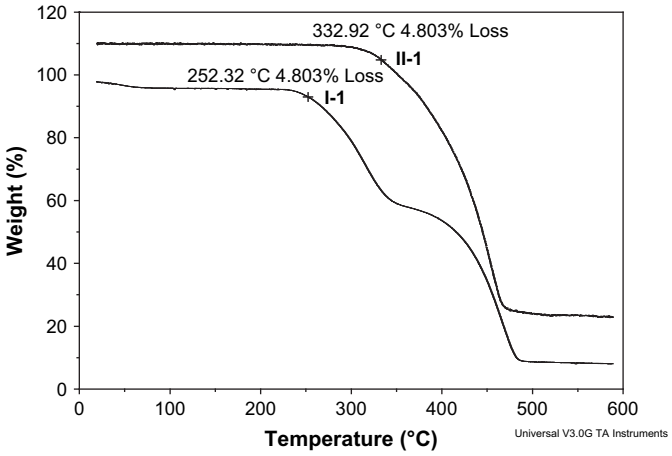

Fig. 7. TGA plots of polymer **I-1** and polymer **II-1** obtained at a heating rate of 10 °C/min in nitrogen.

main chain were conducive to the thermotropic LC property of polymer **I-1** because of the significant reduction of strong ionic interactions between positive and negative charges, which is in excellent agreement with the results of other ionic polymers [23–26].

The DSC thermograms of polymer **II-1** are displayed in Fig. 5b. In the first heating cycle, it showed a weak T_g and a small endotherm ($\Delta H = 0.32$ kcal/mol) with a peak maximum at 148 °C. It showed a distinct T_g at 105 °C in the second heating cycle, but showed a slightly lower T_g (100 or 90 °C) in each of the cooling cycles like that of polymer **I-1**. At the temperature of ca. 150 °C (T_m) it formed a very viscous melt, but there was no development of identifiable LC texture. However, it showed occasionally very small birefringent domains on shearing suggestive of its LC phase. Attempts on annealing even for 2–3 days were failed to develop LC texture of polymer **II-1**. The non-identifiable texture of LC phase also precluded one to determine its T_i. When compared with polymer **I-1**, it showed excellent thermal stability up to 333 °C (Fig. 7) obtained under essentially identical conditions. Its T_m was lower than that of polymer **I-1**.

Thermal properties of other polymers **I-2**, **II-2**, **I-3** and **II-3** in the series are compiled in Table 4. Polymer **I-2** formed a very viscous melt at 159 °C, which hindered the development of an identifiable texture after immediate melting. However, further heating to a high temperature of 210 °C, it developed distinctly large birefringence and isotropic (dark) domains with increased mobility indicative of its LC phase (Fig. S3a). This LC texture remained up to its T_d. Furthermore, on annealing at 210 °C for 3 h it did not develop the fully birefringence domains. Instead, its large birefringent domains were broken into smaller ones mixed with isotropic domains (Fig. S3b). Polymer **II-2** exhibited a broad endotherm (Table 4), which was related to its crystal-to-LC transition (T_m). It was presumably an overlapped one with T_g and T_m. However, the very viscous nature of this melt hindered the development of identifiable texture after immediate melting, but with further heating to a high temperature of 180 °C or above and then shearing it developed birefringent domains with increased mobility indicative of its LC phase (Fig. S4a). Additionally, on annealing for 2 days at 130 °C, it developed small bâtonnets' texture along with dark background (Fig. S4b) suggestive of its LC phase. This LC texture remained up to a high temperature, but its disappearance for the determination of its T_i was quit problematic.

Table 4
Thermal properties of polymers **I-2**, **II-2**, **I-3** and **II-3**

Polymer		T_g[a] (°C)	T_m[b] (°C)	$T^c_{LC-LC'}$ (°C)	T_i[d] (°C)	T_d[e] (°C)
I-2	1H	100	159[f]		–[g]	253
	2H	91	–			
II-2	1H	–	109[h]		–[i]	310
	2H	92	–			
I-3	1H	70	126[f]	163[f]	–[g]	240
	2H	71	–	–		
II-3	1H	–	105[h]		–[i]	294
	2H	83	–			

[a] Glass transition temperature.
[b] Crystal-to-liquid–crystalline phase transition.
[c] One type of liquid–crystalline to the other type of liquid–crystalline phase.
[d] Isotropic transition.
[e] Decomposition temperature at which 5 wt% loss of polymer occurred at a heating rate of 10 °C/min in nitrogen.
[f] Small endotherm.
[g] Isotropic transition by POM was not detected because of decomposition.
[h] Broad and small endotherm.
[i] Isotropic transition by POM was not detected because of the difficulty in the visualization of disappearance of birefringent domains into isotropic phase.

Polymer **I-3** exhibited two small endotherms with peak maxima at 126 and 163 °C. The small low-temperature endotherm was related to the T_m. However, the highly viscous nature of this melt hindered the development of an identifiable texture at the end of the low-temperature endotherm. Even with further heating to the end of the second endotherm at high temperature of 165 °C, it did not develop the LC texture. However, on annealing for 24 h at 165 °C, it developed large birefringent domains along with dark regions, just like polymer **I-2** (Fig. S5a). This LC texture transformed into small birefringent domains mixed with dark regions (Fig. S5b) when heated up to 235 °C just before its T_d (Table 4). Polymer **II-3** exhibited a small, broad endotherm with a peak maximum at 105 °C in the first heating cycle. Its broad endotherm in the first heating cycle was related to its T_m, which was presumably an overlapped one with T_g and T_m. However, the very viscous nature of this melt hindered the development of identifiable texture after immediate melting, but with further heating to a high temperature of 160 °C or above and then shearing it developed small birefringent domains with increased mobility indicative of its LC phase. Additionally, on annealing for 3 days at 130 °C, it developed small birefringent domains mixed with dark background suggestive of its LC phase. This LC texture remained up to a high temperature, but its disappearance for the determination of its T_i was far from satisfactory.

The nature or LC phase (nematic or smectic) for each of these polymers **I-1–I-3** and **II-1–II-3** was found to be the smectic phase, since Fig. 6 (and Figs. S3–S5) shows small and/or large bâtonnets in their photomicrographs. Note here that the small or large bâtonnets are the microstructures of low order smectic phases (S_A or S_C) [48,49]. The biphasic textures of birefringent and isotropic domains observed in polymers **I-2** and **I-3**, when compared with polymer **I-1**, were presumably related to the dilution of LC forming units with the more flexible units present in these polymers. Similar results were also reported in other neutral polymers such as PPV containing oligo(oxyethylene) units in the side chain [7] and fully aromatic polyesters containing two oligo(oxyethylene) units in the side chain [50] and semiflexible aromatic polyesters containing oligo(oxyethylene) units in the main chain [51].

The smectic-to-isotropic phase transition (T_i) for each of the polymers **II-1–II-3** was not detected by DSC measurement presumably because of the broadness of this transition that occurs frequently in many polymers [23,24]. Attempts

to determine this transition for each of these polymers by POM studies also failed, since the observation of the disappearance of weak birefringence phase was quite problematic. In general, polymers **I-1**–**I-3** had higher T_m values than those of polymers **II-1**–**II-3**. Furthermore, they did not exhibit T_i, that is, their LC phase persisted up to their decomposition temperatures. Although T_i values of **II-1**–**II-3** were not measured, but they were far below their decomposition temperatures, all of them had low T_m values and very high thermal stability. These results suggested that the triflimide as counterions in polymers **II-1**–**II-3** not only decreased the T_m but also the T_i. The reason for both the low T_m and low T_i values of these polymers originates partly from a recently reported crystal structure of 1-benzyl-2-ethyl-3-methyl imidazolium triflimide salt. The negative charge delocalization expected in this organic counterion extends only from the central nitrogen to the neighboring sulfur atoms and not to any great extent onto four sulfonyl oxygen atoms. The result of this partial delocalization through pπ–dπ interactions is that the negative charge is significantly buried within the anion and shielded by four oxygen atoms and two terminal $-CF_3$ groups from Coulomb interactions with the neighboring cations. These reduced interactions, therefore, appear to be associated with the increased ion mobility and reduced lattice energy in the crystalline state [52,53]. Thus, it was reasonable to assume that the reduced ionic interactions between triflimide and 4,4′-(1,4-phenylene)bis(2,6-diphenylpyridinium) ions in these polymers, as are similar to the ionic salt (*vide supra*), provided a unique mechanism for their low T_m and low T_i.

The T_d values of polymers **I-1**–**I-3** and **II-1**–**II-3** were determined by TGA measurement at a heating rate of 10 °C/min in nitrogen. All polymers had relatively high T_d values in the range 241–333 °C, which could be useful for processing at relatively low temperatures. The differences of T_d values of **I-1** and **II-1**, of **I-2** and **II-2**, and of **I-3** and **II-3** were 80, 57 and 54 °C, respectively. The steady decrease in T_d values was related to the more flexibility of oxyalkylene units in the polymer chains. The more flexibility of oxyalkylene units in the series of these polymers caused lowering of the T_d value. In general, polymers **II-1**–**II-3** having triflimide counterions showed consistently higher T_d values of over 50 °C than the polymers with tosylate counterions. These results are in excellent agreement with the thermotropic LC properties of other main-chain ionic polymers containing triflimide as counterions [23,25].

3.7. UV–vis and photoluminescence properties

Because all of the polymers **I-1**–**I-3** and **II-1**–**II-3** contained 4,4′-(1,4-phenylene)bis(2,6-diphenylpyridinium) ions in the main chain that act as chromophores, they were examined for their optical properties both in solution and in the solid state. As a representative example, Fig. S6 shows the UV–vis spectra of polymers **I-1** and **II-1** in DMSO ($\varepsilon = 48.9$) recorded at room temperature. Both the polymers displayed absorption maximum (340 nm) in their UV–vis spectra in this polar solvent. However, their λ_{max} values were located at 335 nm in slightly less polar solvents such as acetonitrile ($\varepsilon = 37.5$) and methanol ($\varepsilon = 32.6$) (not shown). The λ_{max} values of polymers **I-1**–**I-3** and **II-1**–**II-3** in polar organic solvents were collected from their absorption spectra and are compiled in Table 5. The bathochromic shift in their λ_{max} values with the increase in relatively low polar solvent to high polar solvent suggested that all of these absorption maxima were indicative of closely spaced π–π* transitions common to aromatic rings. A model compound what is known as 1,2,4,6-tetraphenylpyridinium perchlorate exhibits essentially an identical absorption spectrum with a $\lambda_{max} = 312$ nm in ethanol. The absorption band of *ortho*-substituted pyridinium salt consists of two electronic transitions that are intramolecular charge transfer complexes of the 2,6- and the 4-substituent with the positively charged nitrogen center [54]. Thus, it was reasonable to state that the absorption bands of all of these polymers arose from the same electronic transitions as those in closely related pyridinium salts.

Fig. 8a shows the photoluminescence spectra of polymer **I-1** at various concentrations in methanol, acetonitrile and DMSO. The emission spectra of polymer **I-1** in methanol (2.63×10^{-6} M) and acetonitrile (6.57×10^{-7} M) gave an identical λ_{em} peak at 445 nm at excitation wavelengths of 325 and 330 nm, respectively. However, at much higher concentration (1.58×10^{-3} M) in DMSO its emission spectrum showed a λ_{em} peak at 584 nm at excitation wavelength of 410 nm, since its λ_{em} peak could not be measured at the identical concentrations in methanol and acetonitrile. Its light emission at dilute concentration in this solvent was too weak to measure. However, there were λ_{ex} peak maxima at 333, 323 and 437 nm in methanol, acetonitrile and DMSO solutions when monitored at wavelengths 445, 445 and 585 nm, respectively, in its excitation spectra. Furthermore, the intensity of light emission from DMSO solution was less intense than that from either methanol or acetonitrile (Fig. 8a). Fig. 8b shows the emission spectra of thin films of polymer **I-1** cast from methanol, acetonitrile and DMSO when excited at an identical wavelength of 345 nm. As were similar to solution spectra in methanol and acetonitrile, its film cast from these solvents also exhibited a single λ_{em} peak at 488 nm at excitation wavelength of 345 nm. At various other excitation wavelengths its film also emitted light of ca. 488 nm with varying intensity (not shown). However, the film cast from DMSO gave a λ_{em} peak at 514 nm at an excitation wavelength of 345 nm. It also emitted light of ca. 514 nm of varying intensity

Table 5
UV–vis absorption maxima of polymers **I-1**–**I-3** and **II-1**–**II-3** in various organic solvents

Polymer	λ_{max} (nm)		
	DMSO	CH_3CN	CH_3OH
I-1	340	335	335
II-1	340	335	335
I-2	340	330	330
II-2	340	330	330
I-3	335	330	330
II-3	335	330	330

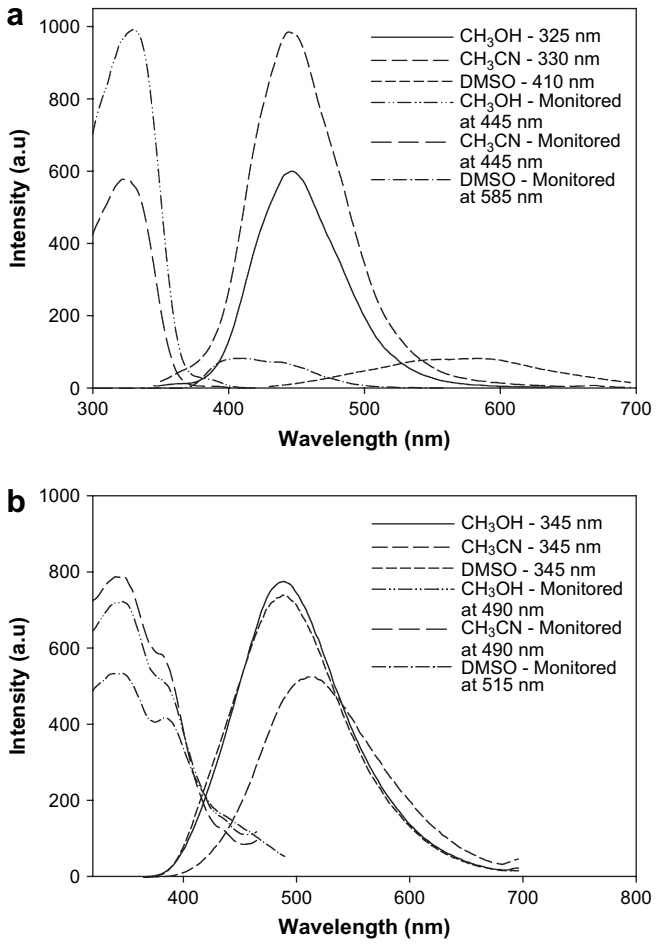

Fig. 8. Emission spectra of polymer **I-1** at various excitation wavelengths: (a) in methanol, acetonitrile and DMSO solutions and (b) in thin films cast from methanol, acetonitrile and DMSO.

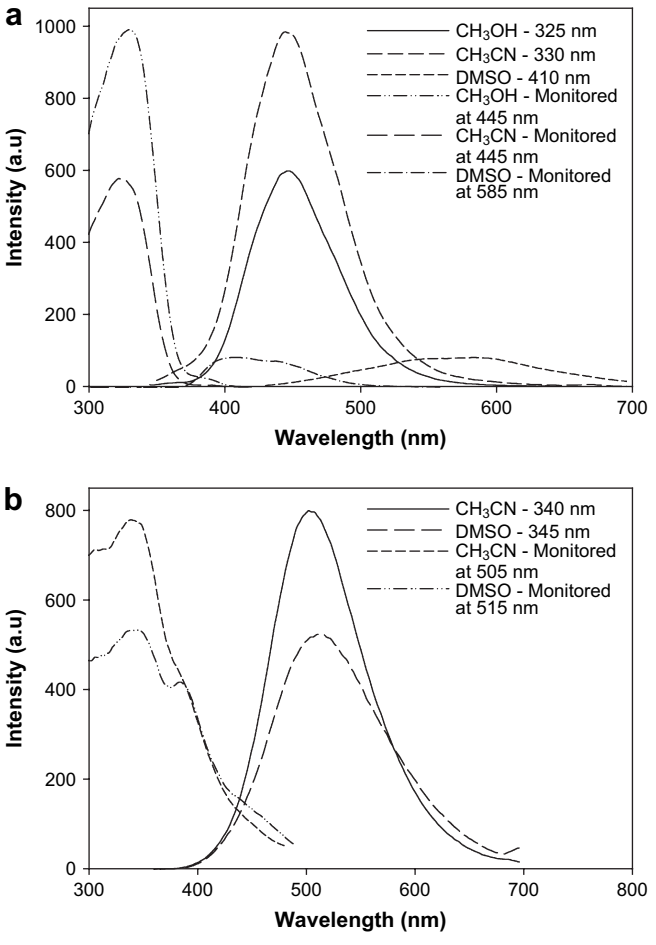

Fig. 9. Emission spectra of polymer **II-1** at various excitation wavelengths: (a) in methanol, acetonitrile and DMSO solutions and (b) in thin films cast from acetonitrile and DMSO.

at other excitation wavelengths (not shown). The films cast from methanol, acetonitrile and DMSO exhibited λ_{ex} peaks at 346 and 384 nm, when monitored at wavelength of 490, 490 and 515 nm, respectively. When compared the solution spectra of polymer **I-1** to the thin film spectra, there was a significant bathochromic shift of 43 nm in both methanol and acetonitrile films, but there was a significant hypsochromic shift of 70 nm in DMSO-cast film.

Fig. 9a shows the photoluminescence spectra of polymer **II-1** at various concentrations in methanol, acetonitrile and DMSO. The emission spectra of polymer **II-1** in methanol (2.14×10^{-6} M) and acetonitrile (5.34×10^{-7} M) gave an identical λ_{em} peak at 446 nm at excitation wavelengths of 325 and 330 nm, respectively. However, at much higher concentration (1.28×10^{-3} M) in DMSO its emission spectrum showed two λ_{em} peaks at 553 and 584 nm at excitation wavelength of 410 nm. The λ_{em} peak of polymer **II-1**, like polymer **I-1**, could not be measured at the identical concentrations in methanol and acetonitrile, since its light emission from such a very dilute concentration in DMSO was also too weak to measure. However, there were λ_{ex} peak maxima at 330, 322 and 437 nm in methanol, acetonitrile and DMSO solutions when monitored at wavelengths 445, 445 and 585 nm, respectively, in its excitation spectra. Additionally, the intensity of light emission from DMSO solution was less intense than that from either methanol or acetonitrile, like that of polymer **I-1** (Fig. 9a).

The films of polymer **II-1** were prepared from their respective solutions in acetonitrile or DMSO casting onto quartz plates. The solid-state emission spectra of polymer **II-1** cast from acetonitrile and DMSO solutions are shown in Fig. 9b. In thin film, it showed a λ_{em} at 502 nm at excitation wavelength 340 nm when cast from acetonitrile solution, but it showed a single λ_{em} at 514 nm at excitation wavelength 345 nm when cast from DMSO solution. On changing from acetonitrile solution to the thin film of polymer **II-1** cast from acetonitrile, there was a significant bathochromic shift of 56 nm in its λ_{em} value, when compared with that of solution spectrum. In contrast, its cast film from DMSO solution exhibited a significant hypsochromic shift of 39 or 68 nm, when compared with that of solution spectrum. Similarly, the light emission from solutions and films cast from various organic solvents of polymers **I-2**–**II-3** was recorded in this study. These polymers in the solid state, like polymers **I-1** and **II-1**, exhibited a similar bathochromic shift in methanol- or acetonitrile-cast films, but exhibited a similar hypsochromic

Table 6
The emission peak maxima of polymers **I-1**–**I-3** and **II-1**–**II-3** in both solutions and films

Polymer	Solvent	λ_{em} (nm)		Polymer concentration (M)
		In solution	In film	
I-1	Methanol	445	488	2.63×10^{-6}
I-1	Acetonitrile	445	488	6.57×10^{-7}
I-1	DMSO	584	514	1.58×10^{-3}
II-1	Methanol	446	–[a]	2.14×10^{-6}
II-1	Acetonitrile	446	502	5.34×10^{-7}
II-1	DMSO	582, 553	514	1.28×10^{-3}
I-2	Methanol	446	488	2.51×10^{-6}
I-2	Acetonitrile	446	491	9.42×10^{-7}
I-2	DMSO	584	509	7.15×10^{-3}
II-2	Methanol	447	–[a]	7.03×10^{-6}
II-2	Acetonitrile	447	501	5.15×10^{-7}
II-2	DMSO	582, 551	494	7.24×10^{-3}
I-3	Methanol	442	501	7.16×10^{-6}
I-3	Acetonitrile	443	–[a]	7.24×10^{-8}
I-3	DMSO	585, 545	497	7.39×10^{-3}
II-3	Methanol	444	–[a]	9.6×10^{-7}
II-3	Acetonitrile	442	478	2.41×10^{-7}
II-3	DMSO	573, 544	487	4.28×10^{-7}

[a] Intensity of light emission was too weak to measure in this film.

shift in DMSO-cast films. The intensity of light emission of these polymers from DMSO solutions was qualitatively lower than that from methanol or acetonitrile solutions (Figs. 8a and 9a). In contrast, the DMSO-cast films of these polymers had comparable intensity of light emission to those in methanol- or acetonitrile-cast films (Figs. 8b and 9b). The λ_{em} peak maxima for all of these polymers in both solutions and films are compiled in Table 6. Furthermore, polymers **II-1**–**II-3** also exhibited light emission ca. 445 nm from relatively nonpolar solvent such tetrahydrofuran ($\varepsilon = 7.6$) and acetone ($\varepsilon = 20.6$). The acetone-cast films of polymers **II-2** and **II-3** exhibited a bathochromic shift of 52 and 43 nm, respectively, when compared with their solution spectra (not shown).

The bathochromic shift in the light emission from films of all of these polymers strongly suggests that there existed more ordered structures in the solid-state films cast from methanol or acetonitrile. In contrast the hypsochromic shift in the light emission from films of all of these polymers strongly suggests that there were less ordered structures in the solid-state films of these polymers, irrespective of the nature of organic counterions used in this study. Both intra- and intermolecular π–π interactions of chromophores are mainly responsible for these ordered structures, which in turn usually cause both to shift λ_{em} peak bathochromically and to lower the quantum yields of light-emitting polymers in the solid state [55,56].

4. Conclusions

Several poly(pyridinium salt)s with tosylate and triflimide as counterions were prepared by either the ring-transmutation polymerization of phenylated bis(pyrylium tosylate) salt with oxyalkylene diamine in dimethyl sulfoxide or the metathesis reaction of the corresponding tosylate polymer with lithium triflimide in methanol. They were characterized for their lyotropic and thermotropic liquid–crystalline properties with various experimental techniques. Polymer **I-1** exhibited a lyotropic liquid–crystalline phase in acetonitrile. Its C^* for the formation of biphasic solution and concentration for the formation of lyotropic phase were 20 and 70 wt% in acetonitrile, respectively. Polymers (**I-1**–**I-3**) with tosylate as counterions exhibited smectic liquid–crystalline phases at relatively low temperatures that persisted up to their decomposition temperatures. The corresponding polymers (**II-1**–**II-3**) with triflimide as counterions had not only low T_m values but also low T_i values, which were well below their decomposition temperatures, exhibiting a broad temperature range of LC phase. Generally triflimide containing polymers also had better thermal stability than the tosylate polymers. They are the novel members of a class of poly(pyridinium salt)s that exhibited both lyotropic and thermotropic liquid–crystalline properties, which can be classified as amphotropic polymers. Although the literature is replete with many lyotropic (solvent induced) and many thermotropic (heat induced) liquid–crystalline polymers, relatively few amphotropic liquid–crystalline polymers both neutral and ionic polymers exist to date [14,57–60].

All of them exhibited light-emitting properties both in polar organic solvents and in the solid state. For example, polymer **I-1** emitted light of wavelength 445 nm from methanol and 584 nm from dimethyl sulfoxide solutions. In its thin film cast from methanol, the wavelength of light emission was shifted bathochromically to 488 nm, because of the ordered structures in the solid state.

The combination of lyotropic liquid–crystalline, thermotropic liquid–crystalline property, the ease of film formation, and photoluminescence makes these polymers interesting for optoelectronic applications such as polymer light-emitting devices, especially linearly polarized light emission. They are also ideal cationic polyelectrolytes for the preparation of multilayer assemblies with controlled morphologies at a molecular level by the sequential deposition technique with anionic polyelectrolytes.

Acknowledgements

P.K.B. acknowledges the University of Nevada at Las Vegas (UNLV) for start-up, Stimulation, Implementation, Transition and Enhancement (SITE), New Investigation Award (NIA), and Planning Initiative Award (PIA), and Applied Research Initiative (ARI) grants, and the Donors of the Petroleum Research Fund, administered by the American Chemical Society, and an award from Research Corporation for the support of this research. A.K.N. acknowledges the Graduate College (UNLV) for providing him a Nevada Stars Graduate Assistantship.

Appendix. Supplementary data

The ^1H and ^{13}C NMR spectra of polymers **I-1** and **II-1** (Figs. S1 and S2), POM photomicrographs of polymers **II-1**, **II-2** and **I-3** (Figs. S3–S5), and UV–vis spectra of polymers

I-1 and **II-1** (Fig. S6) are provided as supplementary material. The supplementary material associated with this article can be found in the online version at, doi:10.1016/j.polymer.2008.02.021.

References

[1] Meng H, Li Z, editors. Organic light-emitting materials and devices. Philadelphia: Taylor & Francis; 2006 [chapter 1], p. 3.
[2] Liu B, Bazan GC. Opt Eng 2005;94:179.
[3] Akcelrud L. Prog Polym Sci 2003;28:875.
[4] Pei Q, Yang Y. J Am Chem Soc 1996;118:7416.
[5] Lauter U, Meyer WH, Enkelmann V, Wegner G. Macromol Chem Phys 1998;199:2129.
[6] Xiang D, Shen Q, Zhang S, Jiang X. J Appl Polym Sci 2003;88:1350.
[7] Mihara T, Yada T, Koide N. Mol Cryst Liq Cryst 2004;411:421.
[8] Benfaremo N, Sandman DJ, Tripathy S, Kumar J, Yang K, Rubner MF, et al. Macromolecules 1998;31:3595.
[9] Hong K-C, Kim J, Bae J-Y. Polym Bull 2000;44:115.
[10] Cacialli F, Friend RH, Feast WJ, Lovenich PW. Chem Commun 2001:1778.
[11] Grell M, Bradley DDC, Inbasekaran M, Woo EP. Adv Mater 1997;9:798.
[12] Grell M, Bradley DDC. Adv Mater 1999;11:895.
[13] Bhowmik PK, Han H, Nedeltchev AK. Polymer 2006;47:8281.
[14] Bhowmik PK, Han H, Nedeltchev IK. J Polym Sci Part A Polym Chem 2002;40:2015.
[15] Bhowmik PK, Burchett RA, Han H, Cebe JJ. Polymer 2002;43:1953.
[16] Bhowmik PK, Burchett RA, Han H, Cebe JJ. Macromolecules 2001;34:7579.
[17] Bhowmik PK, Burchett RA, Han H, Cebe JJ. J Polym Sci Part A Polym Chem 2001;39:2710.
[18] Bhowmik PK, Molla AH, Han H, Gangoda ME, Bose RN. Macromolecules 1998;31:621.
[19] Bhowmik PK, Han H, Basheer RA. In: Salamone JC, editor. Polymeric materials encyclopedia, vol. 5. Boca Raton, FL: CRC; 1996. p. 3741.
[20] Bhowmik PK, Han H. J Polym Sci Part A Polym Chem 1995;33:1745.
[21] Han H, Bhowmik PK. Trends Polym Sci 1995;3:199.
[22] Han H, Vantine PR, Nedeltchev AK, Bhowmik PK. J Polym Sci Part A Polym Chem 2006;44:1541.
[23] Bhowmik PK, Han H, Nedeltchev AK. J Polym Sci Part A Polym Chem 2006;44:1028.
[24] Bhowmik PK, Han H, Cebe JJ, Nedeltchev IK. Macromolecules 2004;37:2688.
[25] Bhowmik PK, Han H, Cebe JJ, Burchett RA, Sarker AM. J Polym Sci Part A Polym Chem 2002;40:659.
[26] Cheng P, Blumstein A, Subramanyam S. Mol Cryst Liq Cryst 1995; 269:1.
[27] Bhowmik PK, Akhter S, Han H. J Polym Sci Part A Polym Chem 1995;33:1927.
[28] Bhowmik PK, Xu W, Han H. J Polym Sci Part A Polym Chem 1994;32:3207.
[29] Katritzky AR, Tarr RO, Heilmann SM, Rasmussen JK, Krepski LR. J Polym Sci Part A Polym Chem 1988;26:3323.
[30] Katritzky AR, Brownlee RTC, Musumarra G. Tetrahedron 1980;36:1643.
[31] Fuoss RM, Strauss UP. J Polym Sci 1948;3:246.
[32] Fuoss RM. J Polym Sci 1948;3:603.
[33] Onsager L. Ann NY Acad Sci 1949;51:627.
[34] Eisenberg H, Pouyet J. J Polym Sci 1954;13:85.
[35] Cohen J, Priel Z, Rabin Y. J Chem Phys 1988;88:7111.
[36] Scranton AB, Rangarajan B, Klier J. Adv Polym Sci 1995;122:1.
[37] Nyrkova I, Shusharina NP, Khokhlov AR. Macromol Theory Simul 1997;6:965.
[38] Ballauff M, Blaul J, Guilleaume B, Rehahn M, Traser S, Wittemann M, et al. Macromol Symp 2004;211:1.
[39] Moinard D, Borsali R, Taton D, Gnanou Y. Macromolecules 2005;38:7105.
[40] Dobrynin AV, Rubinstein M. Prog Polym Sci 2005;30:1049.
[41] Harris FW, Chuang KC, Huang SAX, Janimak JJ, Cheng SZD. Polymer 1994;35:4940.
[42] Harris FW, Chuang KC, Huang SAX, Janimak JJ, Cheng SZD. Polymer 2000;41:5001.
[43] Donald AM, Windle AH. Liquid crystalline polymers. Cambridge: Cambridge University; 1999. p. 1–310.
[44] El-Nokaly M, Friberg SE, Larsen DW. J Colloid Interface Sci 1984;98:274.
[45] Rosevear FB. J Am Oil Chem Soc 1954;31:628.
[46] Rosevear FB. J Soc Cosmet Chem 1968;19:581.
[47] Candau M, Ballet F, Debeauvais F, Wittmann J-C. J Colloid Interface Sci 1982;87:356.
[48] Demus D, Richter L. Textures of liquid crystals. Weinheim: Verlag Chemie; 1978.
[49] Gray GW, Goodby JW. Smectic liquid crystals: textures and structures. Glasgow: Leonard Hill; 1984.
[50] Lee J-W, Joo S-H, Jin J-I. Macromol Res 2004;12:195.
[51] Hubbard HVStA, Sills SA, Davies GR, McIntyre JE, Ward IM. Electrochim Acta 1998;43:1239.
[52] Golding JJ, MacFarlane DR, Spiccia L, Forsyth M, Skelton BW, White AH. Chem Commun 1998:1593.
[53] MacFarlane DR, Meakin P, Sun J, Amini N, Forsyth M. J Phys Chem B 1999;103:4164.
[54] Makoswski MP, Mattice WL. Polymer 1993;34:1606.
[55] Sarker AM, Strehmel B, Neckers DC. Macromolecules 1999;32:7409.
[56] Gettinger C, Heeger AJ, Drake J, Pine D. J Chem Phys 1994;101: 1673.
[57] Aharoni SM. J Polym Sci Polym Phys Ed 1980;18:1303.
[58] Kaeriyama K, Kouyama S, Sekita M, Nakayama T, Tsukahara Y. Macromol Rapid Commun 1999;20:50.
[59] Mruk R, Prehl S, Zentel R. Macromol Chem Phys 2004;205:2169.
[60] Choi K, Mruk R, Moussa A, Jonas AM, Zentel R. Macromolecules 2005;38:9124.